ULF Wave Activity Observed in the Nighttime Ionosphere Above and Some Hours Before Strong Earthquakes

X. Y. Ouyang, Michel Parrot, J. Bortnik

JGR Space Physics

RESEARCH ARTICLE
10.1029/2020JA028396

ULF Wave Activity Observed in the Nighttime Ionosphere Above and Some Hours Before Strong Earthquakes

X. Y. Ouyang[1], M. Parrot[2], and J. Bortnik[3]

[1]Institute of Earthquake Forecasting, China Earthquake Administration, Beijing, China, [2]University of Orléans, LPC2E/CNRS, Orléans, France, [3]Department of Atmospheric and Oceanic Sciences, University of California, Los Angeles, CA, USA

Key Points:
- Earthquakes correlate closely with ULF wave activity in the nighttime ionosphere
- ULF wave activity in the nighttime ionosphere enhances some hours before earthquakes
- Pre-earthquake ULF wave activity increases in an area with a radius less than 200 km

Correspondence to:
X. Y. Ouyang,
oyxybj@qq.com;
oyxy@ief.ac.cn

Citation:
Ouyang, X. Y., Parrot, M., & Bortnik, J. (2020). ULF wave activity observed in the nighttime ionosphere above and some hours before strong earthquakes. *Journal of Geophysical Research: Space Physics*, *125*, e2020JA028396. https://doi.org/10.1029/2020JA028396

Received 24 JUN 2020
Accepted 26 AUG 2020
Accepted article online 30 AUG 2020

Abstract We examine the relationship between earthquakes and ultralow frequency (ULF) wave activity in the nighttime ionosphere based on the electric field data in the direct current/ULF range observed by the DEMETER satellite over a ~5.5 year period from May 2005 to November 2010. ULF wave activity is identified by an automatic detection algorithm and those which occur on the geomagnetic disturbed days ($Kp > 3$ at any time intervals) are discarded. Only the earthquakes with depth ≤70 km and occurring in the region of $|MLat| < 40°$ are selected. A superposed epoch analysis is performed to study the statistical association between ULF wave activity and the selected earthquakes. The results show that (1) there are clearly temporal and spatial correlations between ULF wave activity and earthquakes whose catalog magnitudes are both ≥4.8 and ≥5.0, and (2) enhanced ULF wave occurrence rate happens ~1 day and 1 week before the earthquakes and at less than 200 km distance from the epicenters.

1. Introduction

Electromagnetic variations associated with earthquakes have been reported as early as 1960s (Moore, 1964), and cover a wide frequency range from direct current (DC) to very high frequency. These electromagnetic effects are primarily taken from either passive/active ground-based observations or satellite measurements. Ground-based observations of electromagnetic disturbances in the ultralow frequency (ULF, $f < 10$ Hz) range are considered as one of the most promising means to monitor precursory signatures with earthquakes, since the larger skin depth is comparable to the depth of earthquakes (e.g., Yumoto et al., 2009). However, there are also intense debates on the relationship between the reported ULF precursory signals and earthquakes (Campbell, 2009; Masci, 2010; Thomas et al., 2009), mainly due to the fact that the generation mechanisms of ULF disturbances are poorly understood and there is a lack of the statistically significance analysis of ULF anomalies. Recent statistical studies have verified the existence of ULF electromagnetic emissions before earthquakes (Bortnik et al., 2008; Han et al., 2014; Hattori et al., 2013).

Theoretical studies have shown that the penetration of electromagnetic emissions induced by earthquakes into the upper ionosphere and magnetosphere is possible only in the ULF range (Molchanov et al., 1995). Several case studies suggest that anomalous ULF wave activity before earthquakes is recorded by satellites in the ionosphere, such as the Swarm and the DEMETER satellites (De Santis et al., 2017; Walker et al., 2013). On the other hand, it is now well established that other ionospheric parameters, for instance, electron/ion density, total electron content, and ELF/VLF wave intensity, have shown pre-earthquake effects (e.g., Liu et al., 2013; Němec et al., 2008; Yan et al., 2017). However, previous studies have not dealt with the statistical relationship between ULF wave activity in the ionosphere and earthquakes.

This study seeks to obtain the large and reliable data set of ULF wave activity in the ionosphere to help address this research gap. The methodology of this study is similar to Bortnik et al. (2008), in which ground-based Pc1 pulsations detected by an automatic identification algorithm are statistically correlated to earthquakes. The remaining part of our paper proceeds as follows: Section 2 describes the list of ULF wave events, detected by an automatic algorithm from electric field data recorded by the DEMETER satellite, and the earthquake catalogs with depth, latitude, and aftershocks under consideration; section 3 shows examples of ULF disturbances before earthquakes; section 4 presents the superposed epoch analysis of ULF wave activity relative to real and random earthquakes; section 5 attempts to test the significance of the correlation; section 6 discusses the association between ULF wave activity in the ionosphere and earthquakes, and section 7 summarizes our conclusions.

2. ULF Wave Events and Earthquake Catalogs

2.1. ULF Wave Events

We use the electric field data in the DC/ULF range observed by the DEMETER satellite from May 2005 to November 2010 to identify ULF wave events in the ionosphere. The DEMETER satellite was launched on 29 June 2004 into a nearly Sun-synchronous circular orbit with a 98° inclination and an altitude of about 710 km, and the altitude was lowered to 660 km in December 2005. Its data are organized per half orbit either on the dayside (~10:30 LT) or nightside (~22:30 LT) at the invariant latitude between −65° and 65° (Lagoutte et al., 2006, p. 2). Three components of electric field data in the DC/ULF range for all operational modes are available with a sampling frequency of 39.0625 Hz and a resolution of ~40 μV/m (Berthelier et al., 2006).

An automatic wave detection algorithm adapted from Bortnik et al. (2007) is applied to the electric field data to identify ULF wave events in the ionosphere, and the detailed description is given in Ouyang et al. (2019). This algorithm consists of two main parts. In the first part, spectral peaks are identified based on the dynamic spectra along each half orbit, which exceed the background spectra by at least 1 order of magnitude. In the second part, spectral peaks in consecutive time segments are grouped into individual wave events. Spectral peaks need to satisfy the conditions of minimum duration (~1 min in our case) and spectral continuity to be treated as an event. In this paper, a finer spatial resolution is needed for analyzing ULF wave activity in the dimension of the distances from epicenters, so we use ~20 s time segments to conduct Fourier transform. Since one sample array of electric field contains 256 data points, there are 20/(256/39.0625) ≈ 3 sample arrays during a 20 s interval. The actual sampling duration $T_s = 256 \times 3/39.0625 = 19.6608$ s, so the consequent frequency resolution $f_s = 1/T_s = 0.0509$ Hz. Therefore, the lower and upper cutoff frequencies are set to 0.0509 and 1 Hz, and the minimum width of the spectral peak is 0.118 Hz ($2f_s$) in our detection algorithm. Since ULF oscillations of electric field recorded by the DEMETER satellite are mostly observed on the nightside (Ouyang et al., 2018), the automatic detection algorithm is only applied to the nightside observations. A total of 64,403 ULF wave events in the nightside ionosphere are obtained during our ~5.5 year period.

2.2. Earthquake Catalogs

According to USGS earthquake catalog (https://earthquake.usgs.gov/earthquakes/search/), there are 18,739 earthquakes with magnitudes larger than or equal to 4.8 from May 2005 to November 2010. In order not to mix pre-earthquake and postearthquake effects, "aftershocks" are not considered in this study. We check the earthquake list chronologically to remove "aftershocks," which are defined as any other earthquakes occurring within the next 15 days almost at the same location of the checked earthquake. The same location of a given earthquake is characterized by a small area centered on the epicenter with its latitude ±1° by longitude ±1°. After removing "aftershocks," still 9,420 earthquakes are left. Since the earthquake's depth may also be a critical parameter for anomaly signals, the concern about depth is included. The skin depth of ULF waves is comparable to the depth of earthquakes. According to the frequency range of our wave events (0.0509–1 Hz), it is estimated that the skin depths are around 2–70 km for typical ground conductivity values (Yumoto et al., 2009). In this paper, we assume that ULF electromagnetic signals in the range of 0.0509–1 Hz from those earthquakes with depth >70 km cannot come out from the lithosphere, so earthquakes with depth >70 km are discarded. Consequently, there remains 7,164 earthquakes with magnitude ≥4.8 in the list. ULF wave activity in the ionosphere enhances in the region of |MLat| ≥ 40° during geomagnetic storms (Ouyang et al., 2019), and it is generally thought that the ULF wave activity at higher latitudes is more likely related to magnetospheric origins. Thus, we only select the earthquakes in the region of |MLat| < 40° in order to avoid possible effects from the magnetosphere. The final earthquake catalogs include 5,594 and 3,442 earthquakes with magnitude ≥4.8 and ≥5.0, respectively. In addition, two corresponding catalogs are generated by keeping the latitude of real earthquakes but shifting the longitude by 25° westward (Li & Parrot, 2013) and uniformly distributing the earthquake times. Keeping the latitude and shifting the longitude can maintain the pattern of epicenter distribution, since most earthquakes spread over specific areas rather than uniformly distribute throughout the globe. On the other hand, this way of generating random epicenters help try to keep the similar ULF wave activity background for real and random earthquakes. The offset of the longitude makes random earthquakes located at a moderate distance from the real epicenters and outside of the usual anomaly searching range. These two random catalogs are used to compare with the results of real earthquakes.

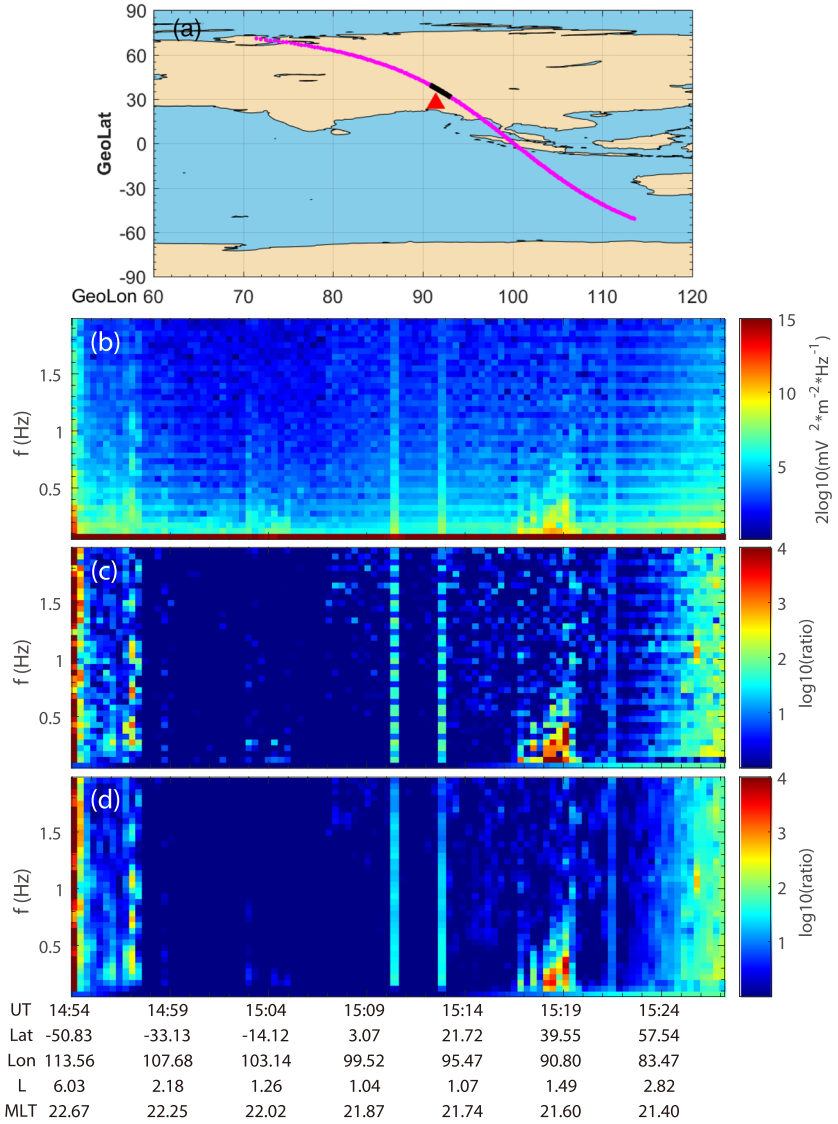

Figure 1. An example of ULF disturbances before the M6.1 Bhutan earthquake on 21 September 2009. (a) The location of the epicenter and a half orbit on 20 September 2009, 1 day before the earthquake; oceans and land in the map are shown in blue and brown, respectively; (b) original dynamic spectra of total cross-covariance power along the half orbit in the panel a; (c) spectra with the background noise removed; and (d) moving averaged spectra.

3. Earthquake Case Study

Figure 1 shows an example of ULF disturbances before the M6.1 Bhutan earthquake (27.33°N, 91.44°E) at 08:53:05 UT on 21 September 2009. We obtain the dynamic spectra of total cross-covariance power of the half orbit (Figure 1b), which is the first step to our automatic wave detection algorithm (Bortnik et al., 2007; Ouyang et al., 2019). As described in Ouyang et al. (2019), the background noise, defined as the median of total cross-covariance power for each frequency component during all time segments along the half orbit, is removed (see Figure 1c); and a moving average is applied to get a smoother spectrogram and better reveal spectral peaks (see Figure 1d). As shown in Figure 1d, ULF disturbances around 15:18 UT last for five consecutive time segments, which have been treated as a ULF wave event. As can be seen from Figure 1a, the location of this ULF wave event indicated in black is very close to the epicenter marked in red. This ULF wave event occurs on a geomagnetic quiet day with $Kp < 3$ and $Dst > -30$ nT at all hours of the day. Another influence factor for ULF wave events is from electron density perturbations which are probably related to plasma irregularities (Ouyang et al., 2018). Thus, we have also checked and found that this ULF

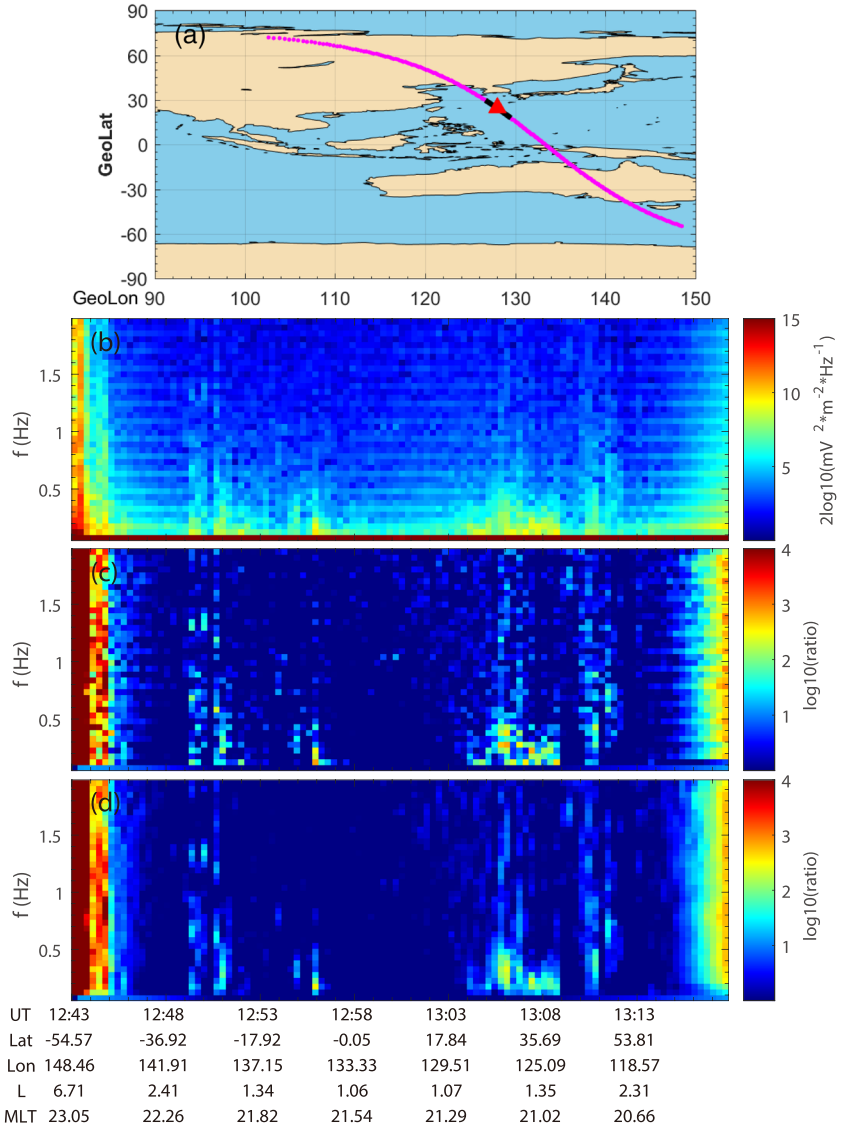

Figure 2. Another example of ULF disturbances before the M5.7 Japan earthquake on 6 July 2009. (a) The location of the epicenter and one half orbit on 6 July 2009, ~10 hr before the earthquake; oceans and land in the map are shown in blue and brown, respectively; (b) original dynamic spectra of total cross-covariance power along the half orbit in the panel a; (c) spectra with the background noise removed; and (d) moving averaged spectra.

wave event is not accompanied by simultaneous electron density perturbations. It is very likely that this ULF wave event has a close association with the M6.1 Bhutan earthquake due to their temporal and spatial correlations.

Another example of ULF disturbances before the M5.7 Japan earthquake (24.87°N, 128.03°E) at 22:35:04 UT on 6 July 2009 is shown in Figure 2. Similar to Figure 1, panels in Figure 2 present the location of the epicenter and the analyzed orbit, original dynamic spectra, spectra with the background removed, and smoothed spectra. Except for disturbances at high latitudes, ULF disturbances from 13:03 to 13:08 UT last for more than 10 consecutive time segments. In addition, the location of these disturbances, which are just above the epicenter, is marked in black in Figure 2a. Same as the example in Figure 1, these ULF disturbances occur on a geomagnetic quiet day and are not accompanied by significantly simultaneous electron density perturbations. This example also demonstrates a very likely correlation between ULF disturbances and the M5.7 Japan earthquake.

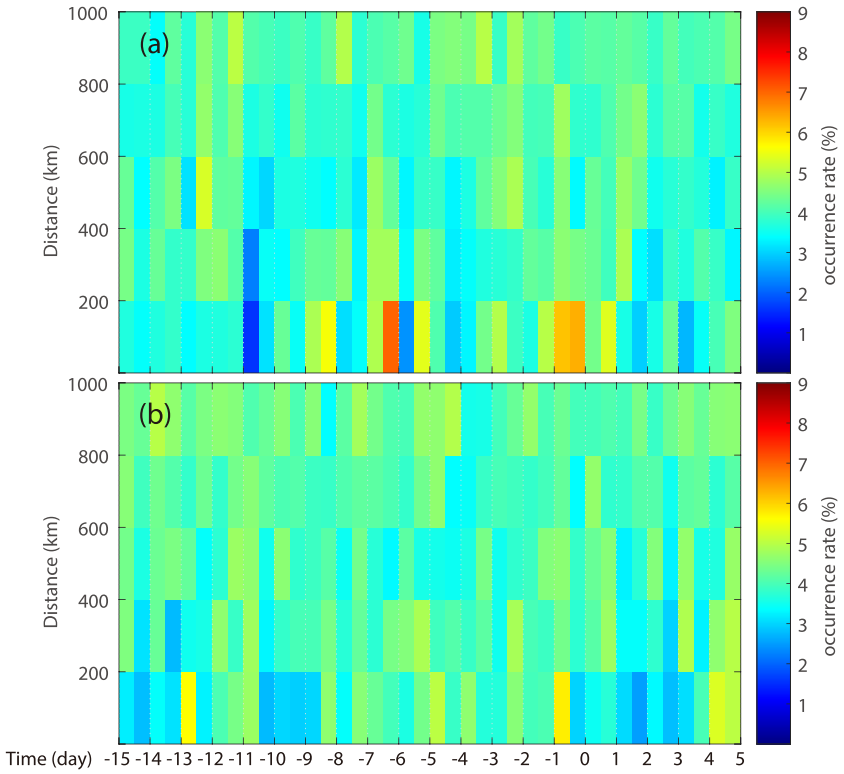

Figure 3. Superposed epoch analysis of ULF wave activity relative to 5,594 earthquakes with magnitudes ≥4.8 and depth ≤70 km in the region of |MLat| < 40°. The occurrence rate of ULF waves is organized in bins of 12 hr (time from the earthquakes) by 200 km (distance from the epicenters). (a) Results of real earthquakes; (b) similar to (a) results of random earthquakes.

4. Superposed Epoch Analysis

To investigate the association between ULF wave activity in the ionosphere and earthquakes, we perform a superposed epoch analysis from 15 days before to 5 days after the earthquake time. Before the superposed epoch analysis, the effects possibly from geomagnetic disturbances need to be eliminated. Therefore, the time periods from 15 days before to 5 days after each earthquake time are checked, if there is a time interval on a day with $Kp > 3$, all wave events on this day are discarded. At least, 45,548 ULF wave events are left for further statistics.

The time difference of each ULF disturbance in each ULF wave event relative to each of the earthquake times and the distance of each ULF disturbance from each of the epicenters are calculated and binned into 12 hr and 200 km bins. The results of the occurrence rate of ULF disturbances relative to real and random earthquakes with magnitudes ≥4.8 and depth ≤70 km in the region of |MLat| < 40° are shown in Figure 3. The occurrence rate is defined as the ratio of the number of ULF disturbance samples to the number of half orbits in each bin. What is interesting in Figure 3a is that ULF wave occurrence rate increases close to the epicenters (less than 200 km) and shortly (~7 and 1 days) before the earthquakes. By contrast, Figure 3b shows results relative to 5,594 random earthquakes. The overall occurrence rate is lower than that in Figure 3a, and it does not show the close temporal and spatial correlations between ULF wave occurrence and the random earthquakes.

Figure 4 shows the superposed epoch results of earthquakes with larger magnitudes (≥5.0). As can be seen from Figure 4a, ULF wave occurrence rate mainly enhances at ~7 and 1 to 2 days before the earthquakes and concentrates in the area of less than 200 km distance from the epicenters, which is similar to the result of earthquakes with magnitudes ≥ 4.8 shown in Figure 3a. As expected, the pre-earthquake effect of ULF wave activity is stronger for results of earthquakes with larger magnitudes. For example, in the bin (−6.5 days, 200 km), the occurrence rate is equal to 6.98% in Figure 3a (magnitudes ≥ 4.8) whereas it is equal to

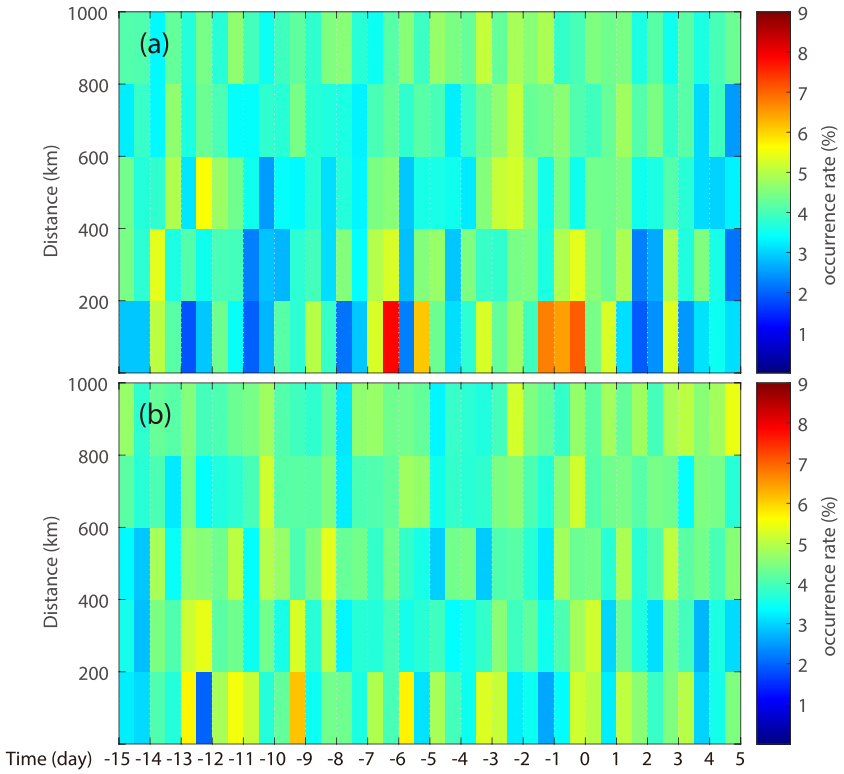

Figure 4. Superposed epoch analysis of ULF waves relative to 3,442 earthquakes with magnitudes ≥5.0 and depth ≤70 km in the region of |MLat| < 40° (similar to Figure 3). (a) Results of real earthquakes and (b) results of random earthquakes.

7.84% in Figure 4a (magnitudes ≥ 5.0). Results of random earthquakes are presented in Figure 4b. The overall occurrence rate in Figure 4b is lower than that in Figure 4a, and it does not show a notable correlation with the earthquakes.

The increase of the ULF wave occurrence rate is relatively small (~2–4%) in Figures 3a and 4a relative to the background. Nevertheless, it is the result of a statistical analysis and ULF waves or oscillations in the ionosphere can be generated by other sources, mainly including ULF waves in the magnetosphere, plasma irregularities in the ionosphere, and lightning in the atmosphere (Ouyang et al., 2019). The two important points are that the occurrence rate is higher than the background close to the epicenters in distance and in time and that this occurrence rate increases with the earthquake magnitude.

5. Significance Test

We have generated two random earthquake sequences with M ≥ 4.8 and M ≥ 5.0 and performed the superposed epoch analysis as shown in Figures 3b and 4b. Since there is no correlation between the random earthquakes and ULF wave occurrence rate, these random earthquake results in Figures 3b and 4b are used to assess the significance of the results in Figures 3a and 4a. All data in Figures 3b and 4b are respectively tested for consistency with a normal distribution using the Kolmogorov-Smirnov test (Massey, 1951), which shows that both are consistent with a normal distribution at the 5%, 1%, and 0.1% significance level. The mean μ and standard deviation σ of each random sequence are derived and used to normalize the results in Figures 3a and 4a. Figures 5a and 5b show the normalized ULF wave occurrence rate, that is, Z value $(= (x - \mu)/\sigma)$, as a function of ΔT and ΔD. It can be seen in Figures 5a and 5b that increase in normalized ULF wave occurrence rate at ΔD < 200 km, ΔT ~ 7 and 1–2 days prior to earthquakes is very significant. Figures 5c and 5d indicate that Z values at ΔD < 200 km are beyond the 0.1% significance level at 6.5 and 0.5 days prior to both M ≥ 4.8 and M ≥ 5.0 earthquakes. The decrease in Z value at ΔT ~ 11 days prior to

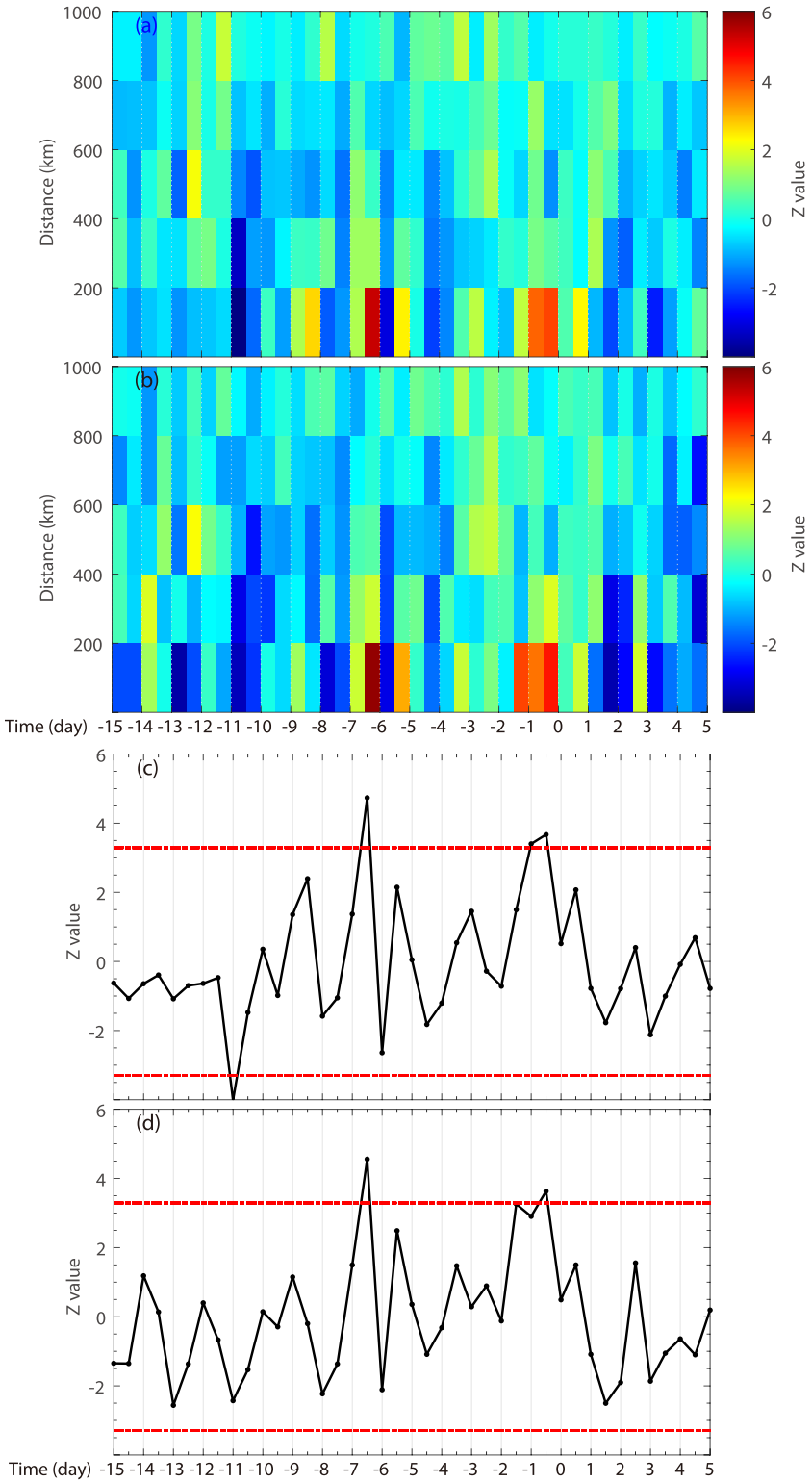

Figure 5. Significance test of ULF wave activity. (a) Normalized ULF wave occurrence rate with respect to M ≥ 4.8 earthquakes, (b) similar to (a) for M ≥ 5.0 earthquakes, (c) normalized ULF wave occurrence rate within 200 km (distance from the epicenters) for M ≥ 4.8 earthquakes, and (d) similar to (c) but for M ≥ 5.0 earthquakes. Red lines at ±3.2905 in (c) and (d) indicate the rejection bounds at the 0.1% significance level.

M ≥ 4.8 earthquakes (Figure 5c) is not taken as an anomaly, since there is not the same phenomenon with respect to M ≥ 5.0 earthquakes (Figure 5d).

6. Discussion

Spacecraft observations of electromagnetic disturbances connected with earthquakes are extensively reported in the ELF/VLF range, with an increase or decrease in the wave intensity (e.g., Němec et al., 2008, and references therein). On the other hand, only a few case studies have tried connecting ULF wave activity with earthquakes (Balasis & Mandea, 2007; De Santis et al., 2017; Walker et al., 2013). In the current statistical study, pre-earthquake effects close to the epicenters are found, suggesting the association between earthquakes and the ULF wave activity as recorded in the ionosphere.

Several models have been suggested for possible generation mechanisms of ULF waves induced by earthquakes, mainly including microfracturing electrification (e.g., Molchanov et al., 2001; Molchanov & Hayakawa, 1995), electrokinetic effect (e.g., Fenoglio et al., 1995; Ishido & Mizutani, 1981; Mizutani et al., 1976; Morgan et al., 1989), and solid state mechanism (e.g., Freund, 2007; Park et al., 1993). Freund (2011) has reviewed some well-known physical processes for seismo-electromagnetic signals, among which, under realistic crustal conditions, microfracturing seems impossible and electrokinetic effect is too weak. Solid state mechanism identifies electronic charge carriers, both electrons and positive holes, which are activated when rocks are stressed and are able to work like a battery. Then sufficiently large electric current could be produced dependent on rock volumes. These electric currents can generate magnetic field variations and low frequency electromagnetic emissions (Freund, 2007, 2011). As shown in Molchanov et al. (1995), the fields from a magnetic type source could penetrate into the upper ionosphere and magnetosphere and the penetration is possible only in the ULF range, which makes it possible to observe ULF wave activity related to earthquakes by satellites.

The spatial scale of significantly enhanced ULF wave activity is less than 200 km as shown in Figures 3a and 4a. According to Dobrovolsky's formula (Dobrovolsky et al., 1979), using the earthquake magnitude, we could estimate the size of earthquake preparation zone. If we calculate the Dobrovolsky's formula for earthquakes with magnitudes ≥4.8 and ≥5.0, we obtain a preparation zone of ~162 and ~196 km, respectively. This estimation well agrees with our results that significant increase in ULF wave occurrence rate happens in the affected area with a radius less than 200 km.

Another important finding is that the time of pre-earthquake effects is at ~7 days and ~1 to 2 days before both for statistical results of earthquakes with magnitudes ≥4.8 (see Figure 3a) and ≥5.0 (see Figure 4a). Previous studies have shown that the decrease of ELF/VLF wave intensity occurs very shortly (<4 hr) before earthquakes (Němec et al., 2008, 2009; Píša et al., 2013). This is not in contradiction with our study because this decrease does not occur in the same frequency range and thus is not related to the same waves. Other ionospheric parameters usually change several days before earthquakes. For example, the statistical studies have reported that ion density perturbations occur 5 days before (Yan et al., 2017); total electron content significantly decrease 2–9 days before (Liu et al., 2013), and abnormal decrease of the ionospheric foF2 occurs within 5 days before the earthquakes (Liu et al., 2006). Our statistical results indicate that the time scale of pre-earthquake ULF disturbances in the ionosphere is similar to other ionospheric parameters.

Our results are obtained from a statistical analysis, and this means that not all earthquakes will trigger ULF oscillations. For example, all earthquakes occurring in the region of |MLat| < 40°, with magnitude >5.5 and depth ≤70 km have been individually studied. For data recorded until 2 days before and at a distance less than 1,000 km from the epicenters, only 34% of these earthquakes present ULF oscillations similar to Figures 1 and 2.

7. Conclusions

This study has examined the association between ULF wave activity in the nighttime ionosphere and earthquakes. ULF wave activity is detected by an automatic algorithm based on the electric field data in the DC/ULF range from May 2005 to November 2010 recorded by the DEMETER satellite. ULF wave events occurring on the geomagnetic disturbed day (Kp > 3 at any time intervals), and earthquakes with depth >70 km or taking place in the region of |MLat| ≥ 40° are discarded. The remaining ULF disturbances

have been statistically correlated to real and random earthquakes with magnitudes ≥4.8 and ≥5.0 during the same period. The major findings are summarized as follows:

1. The superposed analyses have shown the close temporal and spatial correlations between ULF wave activity in the nighttime ionosphere and earthquakes listed in catalogs having magnitudes both ≥4.8 and ≥5.0.
2. The significantly enhanced ULF wave occurrence rate occurs at ~7 and 1 days before the earthquakes and less than 200 km distance from the epicenters. The correlation is stronger for magnitudes ≥5.0 as expected.
3. The test of significance shows that the abovementioned pre-earthquake effects are beyond the 0.1% significance level.

Data Availability Statement

The authors thank the DEMETER scientific mission center for the high-quality data, which can be accessed at https://cdpp-archive.cnes.fr/ website. The *Dst* and *Kp* indices can be accessed at http://wdc.kugi.kyoto-u.ac.jp/wdc/Sec3.html website.

Acknowledgments
This work was supported by the National Key R&D Program of China (2018YFC1503506), the APSCO Earthquake Research Project Phase II, and NSFC grant (41404126). We are grateful to Chao Xiong, Jing Liu, Xuemin Zhang, and Jiehong Chen for their helpful discussions.

References

Balasis, G., & Mandea, M. (2007). Can electromagnetic disturbances related to the recent great earthquakes be detected by satellite magnetometers? *Tectonophysics*, *431*(1–4), 173–195. https://doi.org/10.1016/j.tecto.2006.05.038

Berthelier, J. J., Godefroy, M., Leblanc, F., Malingre, M., Menvielle, M., Lagoutte, D., et al. (2006). ICE, the electric field experiment on DEMETER. *Planetary and Space Science*, *54*(5), 456–471. https://doi.org/10.1016/j.pss.2005.10.016

Bortnik, J., Cutler, J. W., Dunson, C., & Bleier, T. E. (2007). An automatic wave detection algorithm applied to Pc1 pulsations. *Journal of Geophysical Research (1978–2012)*, *112*. https://doi.org/10.1029/2006ja011900

Bortnik, J., Cutler, J. W., Dunson, C., & Bleier, T. E. (2008). The possible statistical relation of Pc1 pulsations to earthquake occurrence at low latitudes. *Annales de Geophysique*, *26*(9), 2825–2836. https://doi.org/10.5194/angeo-26-2825-2008

Campbell, W. H. (2009). Natural magnetic disturbance fields, not precursors, preceding the Loma Prieta earthquake. *Journal of Geophysical Research: Space Physics*, *114*. https://doi.org/10.1029/2008JA013932

De Santis, A., Balasis, G., Pavón-Carrasco, F. J., Cianchini, G., & Mandea, M. (2017). Potential earthquake precursory pattern from space: The 2015 Nepal event as seen by magnetic Swarm satellites. *Earth and Planetary Science Letters*, *461*, 119–126. https://doi.org/10.1016/j.epsl.2016.12.037

Dobrovolsky, I. P., Zubkov, S. I., & Miachkin, V. I. (1979). Estimation of the size of earthquake preparation zones. *Pure and Applied Geophysics*, *117*(5), 1025–1044. https://doi.org/10.1007/bf00876083

Fenoglio, M. A., Johnston, M. J. S., & Byerlee, J. D. (1995). Magnetic and electric fields associated with changes in high pore pressure in fault zones: Application to the Loma Prieta ULF emissions. *Journal of Geophysical Research*, *100*, 12,951–12,958. https://doi.org/10.1029/95JB00076

Freund, F. (2007). Pre-earthquake signals—Part I: Deviatoric stresses turn rocks into a source of electric currents. *Natural Hazards and Earth System Sciences*, *7*(5), 535–541. https://doi.org/10.5194/nhess-7-535-2007

Freund, F. (2011). Pre-earthquake signals: Underlying physical processes. *Journal of Asian Earth Sciences*, *41*(4–5), 383–400. https://doi.org/10.1016/j.jseaes.2010.03.009

Han, P., Hattori, K., Hirokawa, M., Zhuang, J., Chen, C.-H., Febriani, F., et al. (2014). Statistical analysis of ULF seismomagnetic phenomena at Kakioka, Japan, during 2001–2010. *Journal of Geophysical Research: Space Physics*, *119*, 4998–5011. https://doi.org/10.1002/2014ja019789

Hattori, K., Han, P., Yoshino, C., Febriani, F., Yamaguchi, H., & Chen, C.-H. (2013). Investigation of ULF seismo-magnetic phenomena in Kanto, Japan during 2000–2010: Case studies and statistical studies. *Surveys in Geophysics*, *34*(3), 293–316. https://doi.org/10.1007/s10712-012-9215-x

Ishido, T., & Mizutani, H. (1981). Experimental and theoretical basis of electrokinetic phenomena in rock-water systems and its applications to geophysics. *Journal of Geophysical Research*, *86*, 1763–1775. https://doi.org/10.1029/JB086iB03p01763

Lagoutte, D., Brochot, J. Y., & de Carvalho, D. (2006). DEMETER microsatellite scientific mission center data product description. *Demeter*, *1*, 1–79.

Li, M., & Parrot, M. (2013). Statistical analysis of an ionospheric parameter as a base for earthquake prediction. *Journal of Geophysical Research: Space Physics*, *118*, 3731–3739. https://doi.org/10.1002/jgra.50313

Liu, J. Y., Chen, C. H., Tsai, H. F., & Le, H. (2013). A statistical study on seismo-ionospheric anomalies of the total electron content for the period of 56 M ≥ 6.0 earthquakes occurring in China during 1998–2012. *Chinese Journal of Space Science*, *33*(3), 258–269. https://doi.org/10.11728/cjss2013.03.258

Liu, J. Y., Chen, Y. I., Chuo, Y. J., & Chen, C. S. (2006). A statistical investigation of preearthquake ionospheric anomaly. *Journal of Geophysical Research*, *111*. https://doi.org/10.1029/2005ja011333

Masci, F. (2010). On claimed ULF seismogenic fractal signatures in the geomagnetic field. *Journal of Geophysical Research*, *115*. https://doi.org/10.1029/2010JA015311

Massey, F. J. (1951). The Kolmogorov-Smirnov test for goodness of fit. *Journal of the American Statistical Association*, *46*(253), 68–78. https://doi.org/10.1080/01621459.1951.10500769

Mizutani, H., Ishido, T., Yokokura, T., & Ohnishi, S. (1976). Electrokinetic phenomena associated with earthquakes. *Geophysical Research Letters*, *3*(7), 365–368. https://doi.org/10.1029/GL003i007p00365

Molchanov, O., & Hayakawa, M. (1995). Generation of ULF electromagnetic emissions by microfracturing. *Geophysical Research Letters*, *22*(22), 3091–3094. https://doi.org/10.1029/95GL00781

Molchanov, O., Hayakawa, M., & Rafalsky, V. (1995). Penetration characteristics of electromagnetic emissions from an underground seismic source into the atmosphere, ionosphere, and magnetosphere. *Journal of Geophysical Research (1978–2012)*, *100*(A2), 1691–1712. https://doi.org/10.1029/94JA02524

Molchanov, O., Kulchitsky, A., & Hayakawa, M. (2001). Inductive seismo-electromagnetic effect in relation to seismogenic ULF emission. *Natural Hazards and Earth System Sciences*, *1*(1/2), 61–67. https://doi.org/10.5194/nhess-1-61-2001

Moore, G. W. (1964). Magnetic disturbances preceding the 1964 Alaska earthquake. *Nature*, *203*(4944), 508–509. https://doi.org/10.1038/203508b0

Morgan, F. D., Williams, E. R., & Madden, T. R. (1989). Streaming potential properties of westerly granite with applications. *Journal of Geophysical Research*, *94*(B9), 12,449–12,461. https://doi.org/10.1029/jb094ib09p12449

Němec, F., Santolík, O., & Parrot, M. (2009). Decrease of intensity of ELF/VLF waves observed in the upper ionosphere close to earthquakes: A statistical study. *Journal of Geophysical Research (1978–2012)*, *114*. https://doi.org/10.1029/2008JA013972

Němec, F., Santolík, O., Parrot, M., & Berthelier, J. J. (2008). Spacecraft observations of electromagnetic perturbations connected with seismic activity. *Geophysical Research Letters*, *35*. https://doi.org/10.1029/2007GL032517

Ouyang, X. Y., Bortnik, J., Ren, J., & Berthelier, J. J. (2019). Features of Nightside ULF wave activity in the ionosphere. *Journal of Geophysical Research: Space Physics*, *124*, 9203–9213. https://doi.org/10.1029/2019ja027103

Ouyang, X. Y., Zong, Q. G., Bortnik, J., Wang, Y. F., Chi, P. J., Zhou, X. Z., et al. (2018). Nightside ULF waves observed in the topside ionosphere by the DEMETER satellite. *Journal of Geophysical Research: Space Physics*, *123*, 7726–7739. https://doi.org/10.1029/2018JA025248

Park, S. K., Johnston, M. J., Madden, T. R., Morgan, F. D., & Morrison, H. F. (1993). Electromagnetic precursors to earthquakes in the ULF band: A review of observations and mechanisms. *Reviews of Geophysics*, *31*(2), 117–132. https://doi.org/10.1029/93RG00820

Píša, D., Němec, F., Santolík, O., Parrot, M., & Rycroft, M. (2013). Additional attenuation of natural VLF electromagnetic waves observed by the DEMETER spacecraft resulting from preseismic activity. *Journal of Geophysical Research: Space Physics*, *118*, 5286–5295. https://doi.org/10.1002/jgra.50469

Thomas, J. N., Love, J. J., Johnston, M. J. S., & Yumoto, K. (2009). On the reported magnetic precursor of the 1993 Guam earthquake. *Geophysical Research Letters*, *36*. https://doi.org/10.1029/2009GL039020

Walker, S. N., Kadirkamanathan, V., & Pokhotelov, O. A. (2013). Changes in the ultra-low frequency wave field during the precursor phase to the Sichuan earthquake: DEMETER observations. *Annales de Geophysique*, *31*(9), 1597–1603. https://doi.org/10.5194/angeo-31-1597-2013

Yan, R., Parrot, M., & Pinçon, J.-L. (2017). Statistical study on variations of the ionospheric ion density observed by DEMETER and related to seismic activities. *Journal of Geophysical Research: Space Physics*, *122*. https://doi.org/10.1002/2017JA024623

Yumoto, K., Ikemoto, S., Cardinal, M. G., Hayakawa, M., Hattori, K., Liu, J. Y., et al. (2009). A new ULF wave analysis for seismo-electromagnetics using CPMN/MAGDAS data. *Physics and Chemistry of the Earth, Parts A/B/C*, *34*(6–7), 360–366. https://doi.org/10.1016/j.pce.2008.04.005